Biochemical and Biophysical Research Communications 415 (2011) 36–41

Contents lists available at SciVerse ScienceDirect

Biochemical and Biophysical Research Communications

journal homepage: www.elsevier.com/locate/ybbrc

Mxi1 regulates cell proliferation through insulin-like growth factor binding protein-3

Je Yeong Ko [a], Kyung Hyun Yoo [a], Han-Woong Lee [b], Jong Hoon Park [a,*]

[a] Department of Biological Science, Sookmyung Women's University, Seoul, Republic of Korea
[b] Department of Biochemistry, Yonsei University, Seoul, Republic of Korea

ARTICLE INFO

Article history:
Received 24 September 2011
Available online 7 October 2011

Keywords:
Mxi1
IGFBP-3
Proliferation

ABSTRACT

Mxi1, a member of the Myc–Max–Mad network, is an antagonist of the c-Myc oncogene and is associated with excessive cell proliferation. Abnormal cell proliferation and tumorigenesis are observed in organs of Mxi1−/− mice. However, the Mxi1-reltaed mechanism of proliferation is unclear. The present study utilized microarray analysis using Mxi1 mouse embryonic fibroblasts (MEFs) to identify genes associated with cell proliferation. Among these genes, insulin-like growth factor binding protein-3 (IGFBP-3) was selected as a candidate gene for real-time PCR to ascertain whether IGFBP-3 expression is regulated by Mxi1. Expression of IGFBP-3 was decreased in Mxi1−/− MEFs and Mxi1−/− mice, and the gene was regulated by Mxi1 in Mxi1 MEFs. Furthermore, proliferation pathways related to IGFBP-3 were regulated in Mxi1−/− mice compared to Mxi1+/+ mice. To determine the effect of Mxi1 inactivation on the induction of cell proliferation, a proliferation assay is performed in both Mxi1 MEFs and Mxi1 mice. Cell viability was regulated by Mxi1 in Mxi1 MEFs and number of PCNA-positive cells was increased in Mxi1−/− mice compared to Mxi1+/+ mice. Moreover, the IGFBP-3 level was decreased in proliferation defect regions in Mxi1−/− mice. The results support the suggestion that inactivation of Mxi1 has a positive effect on cell proliferation by down-regulating IGFBP-3.

1. Introduction

Mxi1 is an antagonist of the c-Myc oncogene. The Mxi1 gene encodes a protein designated Mad2, which is a basic helix–loop–helix leucine zipper (bHLHzip) transcription factor that belongs to Myc–Max–Mad network. This gene regulates the transcription of a target gene that controls cell proliferation and differentiation [1]. Mxi1 protein dimerizes with Max and binds to consensus E-box elements to regulate various cellular functions in gene promoters [2]. In addition, Mxi1 is located in 10q24-q25, which is a cancer hotspot. This region is mutated and deleted in several cancer types in humans, such as prostate cancers, small-cell lung cancers and renal cell carcinomas. Progressive abnormalities and abnormal cell proliferation are observed in Mxi1-deficient mice [3]. The collective data is consistent with the Mxi1 gene as a tumor suppressor capable of modulating cell proliferation. However, the Mxi1-related proliferation mechanism is unclear. With the aim to clarify this mechanism, microarray analysis was performed using Mxi1+/+ and Mxi1−/− MEFs. The microarray analysis focused on insulin-like growth factor binding protein-3 (IGFBP-3).

Insulin-like growth factor-I (IGF-I) is crucial in the regulation of cell proliferation, apoptosis and differentiation. Growth-promoting activities of IGF-I are regulated by six IGFBPs, which regulate the bioavailability of IGFs in the circulation [4,5]. Among these IGFBPs, IGFBP-3 is the most abundant protein in the extracellular environment. IGFBP-3 binds to IGF-I directly and prevents access of IGF-I to the IGF-I receptor (IGF-IR), which regulates the IGF-dependent pathway that consists of mitogen-activated protein kinase (MAPK) pathway and phosphoinositide 3-kinase (PI3K)-Akt pathway. Consistent with this, IGFBP-3 is thought to be proapoptotic and capable of inhibiting the proliferative effects of IGF-I [6]. IGFBP-3 affects not only the IGF-dependent pathway but also the IGF-independent pathway, such as G1/S transition of the cell cycle. These IGF-dependent and -independent antiproliferative effects of IGFBP-3 have indicated the anticancer potential of IGFBP-3 [7].

The present study provides evidence of the correlation of Mxi1 and IGFBP-3 *in vitro* and *in vivo*. IGFBP-3 is confirmed as an important mediator of the Mxi1-related proliferation mechanism. The proliferation defect caused by inactivation of Mxi1 occurs through IGFBP-3.

Abbreviations: MEF, mouse embryonic fibroblasts; IGFBP-3, insulin-like growth factor binding protein-3.

* Corresponding author. Fax: +82 2 2077 7258.
E-mail address: parkjh@sookmyung.ac.kr (J.H. Park).

0006-291X/$ - see front matter © 2011 Elsevier Inc. All rights reserved.
doi:10.1016/j.bbrc.2011.10.005

2. Materials and methods

2.1. Microarray analysis

Total mRNAs were isolated from Mxi1+/+ and Mxi1−/− MEFs. Microarrays were performed using the AffymetrixGeneChip® Mouse Gene 1.0 ST Array. RNA samples (300 ng) were used as input as recommended by the manufacturer (Affymetrix). Image acquisition utilized an AffymetrixGeneChip® Scanner 3000 7G and Affymetrix GCOS software was used to extract data. Expression data were normalized and log2 transformed using the Robust Multi-array Average (RMA) method. Highly expressed genes that showed a 2-fold change in expression were selected.

2.2. MEF culture

Mxi1+/+ and Mxi1−/− MEFs were isolated from 13.5 day old mouse embryos. Embryos were minced and then dispersed in 0.05% trypsin and then incubated at 37 °C for 15–20 min. MEFs were plated in Dulbecco's Modified Eagle Medium (DMEM) supplemented with fetal bovine serum and then incubated at 37 °C in 5% CO_2.

2.3. Small interfering RNA (siRNA) treatment and transfection

MEFs were treated with Mxi1 siRNA (Santa_Cruz Biotechnology) using LipofectamineRNAi MAX (Invitrogen) according to the manufacturer's protocol. Mxi1 siRNA was used at a concentration of 30 nM and transfection was continued for 48 h. pCMV Tag2B (Stratagene) vector was constructed by cloning Mxi1 cDNA that is isolated from mIMCD-3 (inner medullary collecting duct) and pCMV-SPORT6 vector that contains IGFBP-3 cDNA was purchased from Open Biosystems. MEFs were transfected with Mxi1 and IGFBP-3 using FuGENE HD transfection reagent (Roche) according to the manufacturer's protocol and transfection was continued for 48 h.

2.4. PI staining

MEFs were harvested and washed with PBS and fixed with 70% ethanol. These MEFs were stained using PI/RNase staining buffer (BD Biosciences) according to the manufacturer's protocol and analyzed by BD FACSCanto.

2.5. Real-time polymerase chain reaction (PCR) and semi-quantitative reverse transcription PCR

Total mRNAs were isolated using a Nucleospin® kit (MACHEREY-NAGEL) according to the manufacturer's protocol, and cDNA was synthesized using Moloney murine leukemia virus reverse transcriptase according to manufacturer's instructions (Promega). The results of real time RT-PCR were measured by the real-time PCR SYBR green kit (Qiagen). 2.5 μl of cDNA was mixed with 1 μl of each forward and reverse primer and used to prepare 10 μl of master mix. For real-time PCR, the primers used were: β-actin, forward 5′-GACGATGCTCCCCGGGCTGTATTC-3′, reverse 5′-TCTCTTGCTCTGGGCCTCGTCACC-3′; Mxi1, forward 5′-CGGATTCAGAGCGAGAGGAGATT-3′, reverse 5′-AGGCT GCTGT GGTC GTCAAGGTC-3′; Igfbp-3, forward 5′-GCCG CAGA GAAATGGAGGACAC-3′, reverse 5′-AGGGCGGCACT GCTT CTTCT-3′; Cyclin D1, forward 5′-CGCCAGGCCCAGCAGAAC-3′, reverse 5′-CCGGTGGCCCTCAGATGTC-3′; p57, forward 5′-GAACGCCGAGGACCAGAACC-3′, reverse 5′-GTAGAAGG CGGGCACAGACTCG-3′; Gas1, forward 5′-AGCAGCAGCGGCAGTGGA-3′, reverse 5′-GGG CGCA GGAG CT ACAAGTG-3′. For semi-quantitative RT-PCR, the primers used were: β-actin, forward 5′-CAGGGTGTGATG GTGGGAATG-3′, reverse 5′-ATGGCTGGGGTGTTGAAGGTC-3′; Mxi1, forward 5′-GCAACACCAGCACTGCCAAC-3′, reverse 5′-AGGAGACTGCATCA TGAACC-3′.

2.6. Western blot analysis

Proteins from kidney tissue were separated by SDS–PAGE and transferred to PVDF membranes (Amersham Pharmacia Biotech). These blots were incubated at room temperature with 5% skim

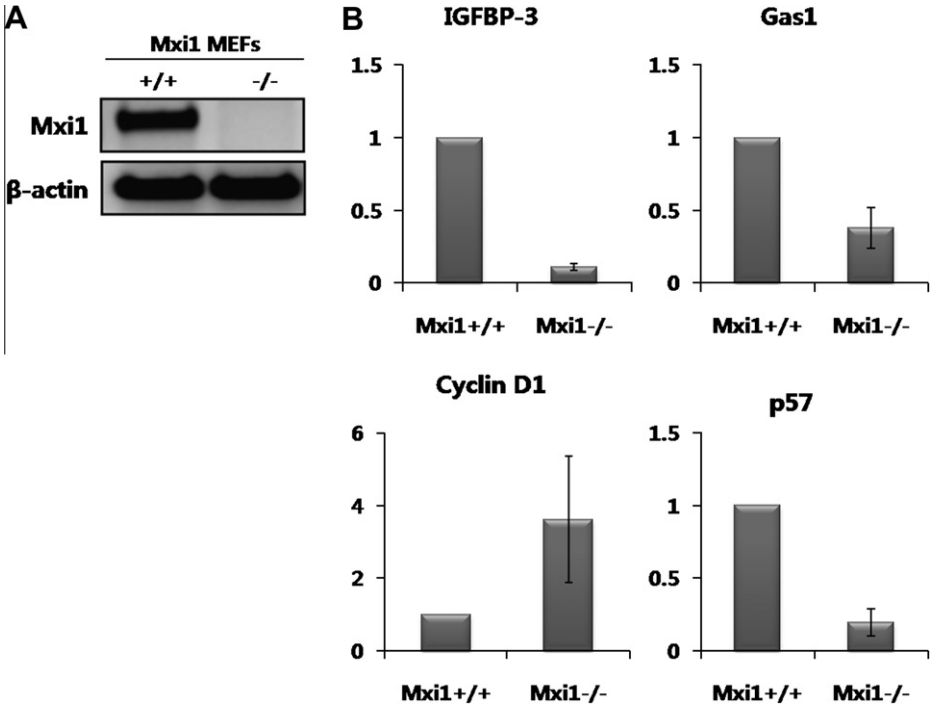

Fig. 1. Verification of genes related to proliferation in microarray analysis of Mxi1 MEFs. (A) Confirmation of Mxi1 expression in Mxi1+/+ and Mxi1−/− MEFs using RT-PCR. (B) Validation of expression of selected genes from microarray data using real-time PCR. Expressions of IGFBP-3 (0.109 ± 0.023), Gas1 (0.38 ± 0.141) and p57 (0.193 ± 0.092) were decreased in Mxi1−/− MEFs. Level of Cyclin D1 (3.616 ± 1.742) was increased in Mxi1−/− MEFs compared to controls.

Table 1
Genes associated with proliferation in microarray analysis of Mxi1 MEFs.

NCBI_No.	Gene description	Fold
NM_007631	Cyclin D1	2.581733
NM_009929	Collagen, type XVIII, alpha 1	0.477564
NM_007833	Decorin	0.375168
NM_016687	Secreted frizzled-related protein 4	0.351967
NM_008343	Insulin-like growth factor binding protein 3	0.333963
NM_010180	Fibulin 1	0.330978
NM_008486	Alanyl (membrane) aminopeptidase	0.308748
NM_008086	Growth arrest specific 1	0.307042
NM_009876	cyclin-dependent kinase inhibitor 1C (P57)	0.2911
NM_010930	Nephroblastoma overexpressed gene	0.225837
NM_016697	Glypican 3	0.162973
NM_008604	Membrane metallo endopeptidase	0.157653

milk for 1 h. Proteins were immunoblotted with primary antibodies against β-actin (Sigma–Aldrich), ERK, p-ERK, Akt, p-Akt, Cyclin D1 and p21 (all from Cell Signaling Technologies).

2.7. Cell proliferation assay

MEFs were seeded at density of 1.0×10^6 cells/well in 6-well plates and the cell viability was measured by an established methyl thiazoyltetrazolium (MTT) assay. MEFs were washed with PBS and incubated with 400 μl of MTT reagent in culture medium at 37 °C for 4 h. These mixture was removed and MEFs were washed with PBS and then 1600 μl of DMSO and 400 μl of glycine buffer per well was added. The absorbance of the converted dye was measured at a wavelength of 570 nm using a Sunrise Remote Microplate Reader.

2.8. Immunohistochemistry

Paraffin sections were deparaffinized with Histo-Clear II (National Diagnostics) and rehydrated with graded enthanols. A VECTROSTAIN ABC kit (Vector Laboratories) was used for immunostaining according to the manufacturer's protocol. Slides were stained by primary

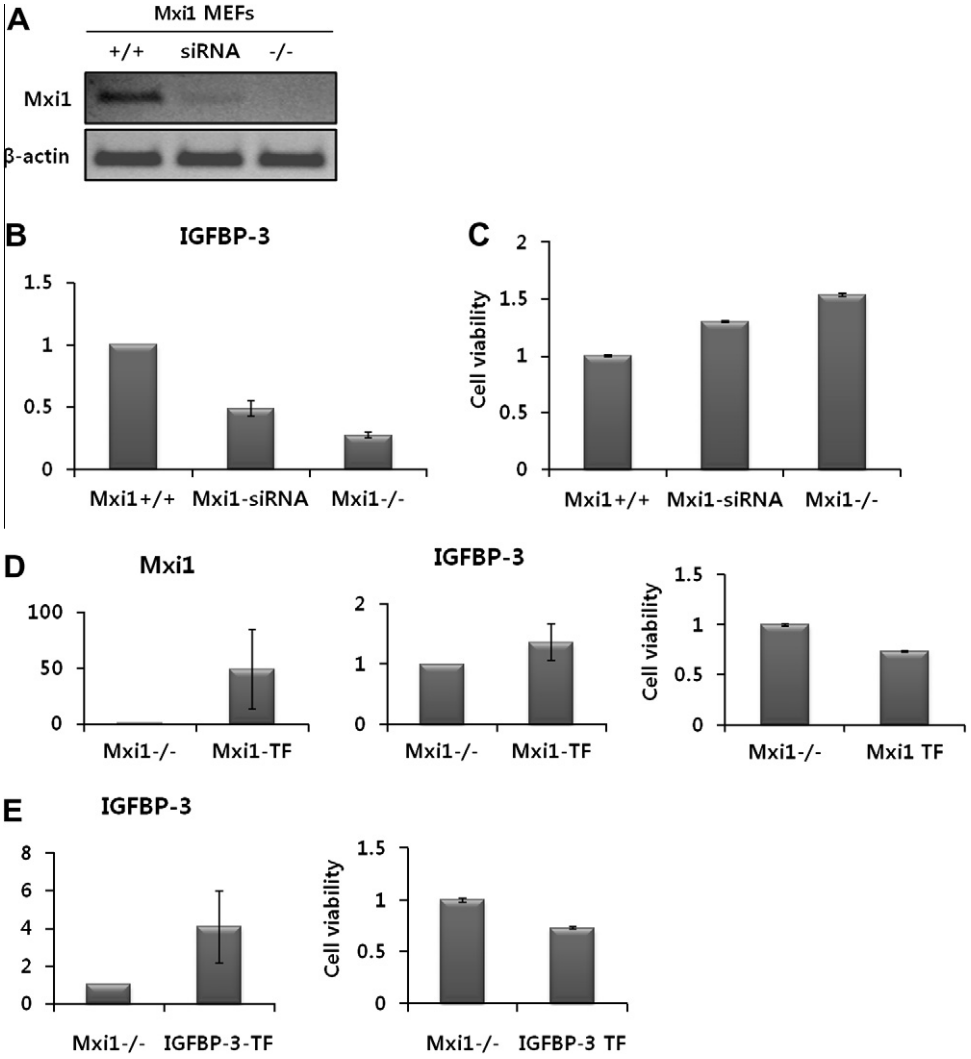

Fig. 2. Effect of Mxi1 on IGFBP-3 expression and cell proliferation. (A) Expression level of Mxi1 was confirmed by RT-PCR in Mxi1+/+, Mxi1-siRNA treated Mxi1+/+ and Mxi1−/− MEFs. (B) Comparison of IGFBP-3 expression in Mxi1+/+, Mxi1-siRNA treated Mxi1+/+ and Mxi1−/− MEFs using real-time PCR. Expression of IGFBP-3 in Mxi1-siRNA treated Mxi1+/+ (0.489 ± 0.064) and Mxi1−/− MEFs (0.271 ± 0.024) was reduced compared to Mxi1+/+ MEFs. (C) Results of the MTT-based cell viability assay. Mxi1 affected proliferation in Mxi1 MEFs. Cell viability of Mxi1-siRNA treated Mxi1+/+ was increased by about 1.3 times (1.302 ± 0.008) compared to Mxi1+/+ MEFs. The proliferation rate of Mxi1−/− MEFs was increased by about 1.5–fold (1.537 ± 0.012) compared with Mxi1+/+ MEFs.(D) Real-time PCR and MTT assay were performed in Mxi1−/− MEFs and Mxi1 transfected Mxi1−/− MEFs. Expression of Mxi1 in Mxi1 transfected Mxi1−/− MEFs (48.449 ± 35.567) was increased compared to controls (left). Expression of IGFBP-3 in Mxi1 transfected Mxi1−/− MEFs (1.367 ± 0.300) was increased compared to controls (middle). Cell viability of Mxi1 transfected Mxi1−/− MEFs (0.733 ± 0.006) was decreased compared to controls (right). (E) Real-time PCR and MTT assay were performed in Mxi1−/− MEFs and IGFBP-3 transfected Mxi1−/− MEFs. Expression of IGFBP-3 in IGFBP-3 transfected Mxi1−/− MEFs (4.073 ± 1.928) was increased compared to controls (left). Cell viability of IGFBP-3 transfected Mxi1−/− MEFs (0.730 ± 0.014) was decreased compared to controls (right).

antibodies to PCNA and IGFBP-3 (both from Santa Cruz Biotechnology) and incubated overnight at 4 °C. Immunoreactive signals were visualized by NovaRed (Vector Laboratories).

3. Results

3.1. Validation of genes associated with proliferation in Mxi1−/− MEFs

To identify the Mxi1-related mechanism of proliferation, microarray analysis was performed using Mxi1+/+ and Mxi1−/− MEFs. The Mxi1 level of the samples used for the microarray was confirmed by RT-PCR (Fig. 1A). A comparison of the pattern of gene expression between Mxi1+/+ and Mxi1−/− MEFs revealed 116 up-regulated genes and 242 down-regulated gene. Table 1 summarizes the proliferation-related genes identified from microarray analysis. Genes involved in growth suppression were decreased and growth promotion genes were increased in Mxi1−/− MEFs compared to controls. Among these genes, real-time PCR was performed to validate the level of genes including IGFBP-3, Gas1, Cyclin D1 and p57 (Fig. 1B). Levels of IGFBP-3, Gas1 and p57 were decreased in Mxi1−/− MEFs, but expression of Cyclin D1 was increased compared to Mxi1+/+ MEFs. Based on these results, IGFBP-3 was selected as a candidate gene because of the markedly decreased level of this gene in Mxi1−/− MEFs.

3.2. Mxi1 regulates IGFBP-3 expression and affects cell proliferation in vitro

To confirm whether Mxi1 regulates IGFBP-3 expression, Mxi1+/+ MEFs were treated with Mxi1 siRNA. The treatment significantly decreased Mxi1 mRNA level compared to Mxi1+/+ MEFs (Fig. 2A). After checking the expression of Mxi1 in Mxi1+/+, Mxi1-siRNA treated Mxi1+/+ and Mxi1−/− MEFs, real-time PCR was undertaken to check the expression of IGFBP-3 in these three cell lines (Fig. 2B). The expression of IGFBP-3 was decreased in Mxi1-siRNA treated Mxi1+/+ MEFs compared to Mxi1 +/+ MEFs. Also, the IGFBP-3 level of Mxi1−/− MEFs was reduced compared with Mxi1-siRNA treated Mxi1+/+ MEFs. The MTT assay was performed in Mxi1+/+, Mxi1-siRNA treated Mxi1+/+ and Mxi1−/− MEFs to confirm the effect of Mxi1 on cell proliferation (Fig. 2C). Cell viability of Mxi1−/− MEFs was increased compared to Mxi1+/+ MEFs, and Mxi1-siRNA treated Mxi1+/+ MEFs had a tendency to induce cell proliferation compared to Mxi1+/+ MEFs. In addition, Mxi1 transfected to Mxi1−/− MEFs to confirm the effect of Mxi1 on IGFBP-3 expression and cell proliferation in Mxi1−/− MEFs, so real-time PCR and MTT assay were performed in Mxi1−/− and Mxi1 transfected Mxi1−/− MEFs (Fig. 2D). When Mxi1 was overexpressed in Mxi1−/− MEFs, IGFBP-3 level was increased and cell viability was decreased. To confirm whether overexpression of IGFBP-3 has a effect on proliferation in Mxi1−/− MEFs, we transfected IGFBP-3 to Mxi1−/− MEFsand performed MTT assay in IGFBP-3 transfected Mxi1−/− MEFs (Fig. 2E). When IGFBP-3 was overexpressed in Mxi1−/− MEFs, cell viability was decreased compared to Mxi1−/− MEFs. These results were consistent with the Mxi1 modulation of the level of IGFBP-3 to regulate cell proliferation.

3.3. Inactivation of Mxi1 suppresses IGFBP-3 level and regulates the pathway related to IGFBP-3 in vivo

The mRNA level of IGFBP-3 in Mxi1+/+ and Mxi1−/− mice was analyzed to determine whether IGFBP-3 is reduced in not only Mxi1−/− MEFs but also Mxi1−/− mice, so we used kidney samples of Mxi1+/+ and Mxi1−/− mice. IGFBP-3 mRNA expression was decreased in Mxi1−/− mice compared to control mice (Fig. 3A), indicative of Mxi1-mediated regulation of IGFBP-3 expression *in vitro* and *in vivo*. To determine the influence of the inactivation of Mxi1 expression on the pathway related to IGFBP-3, western blot analysis was performed *in vivo* (Fig. 3B). We checked the major molecule of these pathways, IGF-dependent and -independent pathway. The levels of p-ERK, p-Akt and Cyclin D1 were increased in Mxi1−/− mice, but p21, a negative regulator of the cell cycle, was decreased in Mxi1−/− mice compared to Mxi1+/+ mice. In addition, we performed PI staining using Mxi1+/+ and Mxi1−/− MEFs because protein level of cell cycle regulators was changed in Mxi1−/− mice compared to controls (Fig. 3C). The cell cycle was progressed in Mxi1−/− MEFs compared to Mxi1+/+ MEFs. These results provided evidence that pathways associated with IGFBP-3 are regulated in Mxi1−/− mice.

3.4. Abnormal cell proliferation occurs through inactivation of IGFBP-3 in Mxi1−/− mice

Confirmation of the effect of Mxi1 on proliferation defects in Mxi1+/+ and Mxi1−/− mice was obtained in an immunohistochemical experiment. Many PCNA-positive cells were detected in Mxi1−/− mice (Fig. 4A, arrows). The number of PCNA-positive cells was significantly increased in Mxi1−/− mice when compared with controls (Fig. 4B). In addition, the level of IGFBP-3 surrounding cysts was significantly decreased as the result of abnormal cell proliferation in Mxi1−/− mice, whereas strong IGFBP-3 signals were detected in Mxi1+/+ mice (Fig. 4C). These results were consistent with the idea that inactivation of Mxi1 promotes abnormal cell proliferation by reducing the level of IGFBP-3.

4. Discussion

Cancer is caused by uncontrolled cell proliferation. Appropriately, regulation of cell proliferation is a target for cancer therapy.

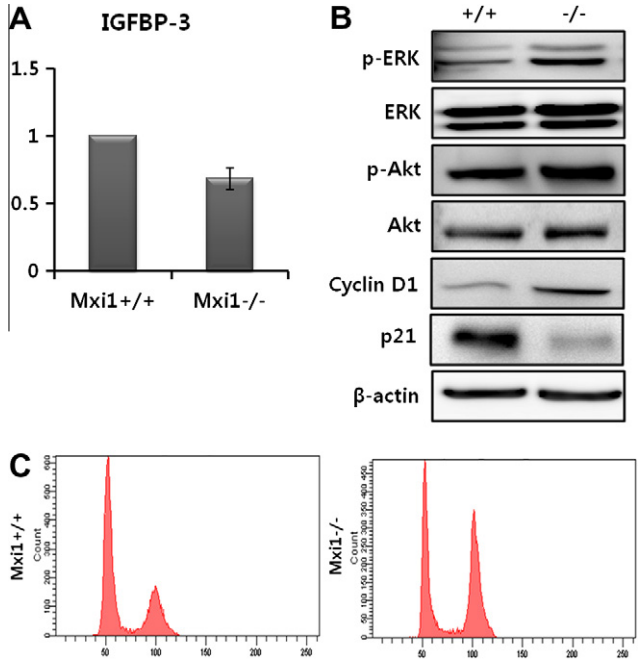

Fig. 3. IGFBP-3 and pathways associated with IGFBP-3 are regulated in Mxi1−/− mice. (A) mRNA expression of IGFBP-3 was reduced in Mxi1−/− mice (0.684 ± 0.078) compared with controls. (B) Pathways associated with IGFBP-3 are IGF-dependent and IGF-independent. IGF-dependent pathway consists of MAPK and PI3K-AKT signaling and G1/S transition molecules of cell cycle belong to IGF-independent pathway. Levels of p-ERK, p-Akt and Cyclin D1 were increased, whereas p21 level was decreased in Mxi1−/− mice compared to control mice. β-actin was used as a loading control. (C) PI staining was performed in Mxi1+/+ and Mxi1−/− MEFs.

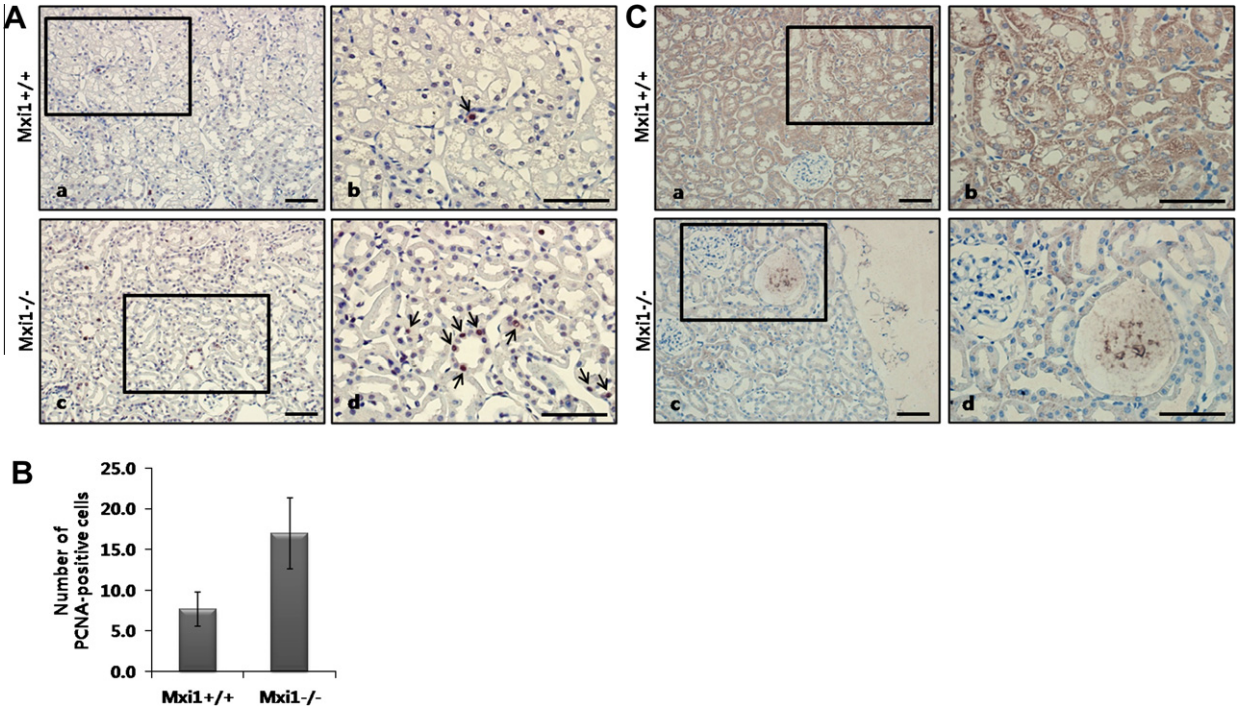

Fig. 4. Verification of PCNA and IGFBP-3 level is performed in Mxi1−/− mice. (A) Confirmation of PCNA-positive cells in kidney samples of Mxi1+/+ (a and b) and Mxi1−/− mice (c and d). PCNA was stained to nucleus of each cell. Many PCNA-positive cells were detected in Mxi1−/− mice. Boxed regions (a and c) are magnified (b and d). Original magnification: 200× (a and c), 400× (b and d); scale bar, 100 μm. (B) Number of PCNA-positive cells was increased about two times in Mxi1−/− mice. (C) Validation of IGFBP-3 expression in kidney samples of Mxi1+/+ (a and b) and Mxi1−/− mice (c and d). IGFBP-3 staining was evident in the cell cytoplasm. Strong IGFBP-3 signals were detected in the kidneys of Mxi1+/+ mice. However, little IGFBP-3 protein was evident surrounding the cysts in Mxi1−/− mice. Boxed regions (a and c) are magnified (b and d). Original magnification: 200× (a and c), 400× (b and d); scale bar, 100 μm.

Inactivation of Mxi1 induces tumors in humans; Mxi1 deletion has been reported in 9–62% of prostate tumors, 12–32% of renal cell carcinomas, 5–26% of meningiomas, 40% of endometrial cancers, 74–91% of small-cell lung cancers, and 13–93% of gliomas [8]. The genetic locus of the Mxi1 gene is related to tumor suppression and Mxi1-deficient mice display abnormal cell proliferation and tumor development [9]. To date, the proliferation mechanism has been unclear, and clarification of this mechanism prompted present study. The present data implicate IGFBP-3 as an effective target for abnormal cell proliferation caused by Mxi1.

IGF-I interacts with IGF-IR to activate the downstream MAPK and PI3K-Akt signaling pathways that are related to proliferation and differentiation [10]. The binding of IGF-I with IGF-IR is regulated by six IGFBPs. Among these, IGFBP-3 is the most abundant and inhibits the interaction of IGF-I with its receptor, so IGFBP-3 suppresses cell proliferation [11]. IGFBP-3 also inhibits angiogenesis by reducing the amount of vascular endothelial growth factor (VEGF) [12]. The high expression of IGFBP-3 is associated with a low risk of cancer, whereas low expression of IGFBP-3 increases the risk of cancer. Thus, IGFBP-3 is an anticancer molecule.

Presently, expression of IGFBP-3 was decreased in Mxi1−/− MEFs and was regulated by the Mxi1 level in Mxi1 MEFs. This correlation was also detected *in vivo*, demonstrating the close relationship between Mxi1 and IGFBP-3. Moreover, both IGF-dependent and -independent pathways were regulated in Mxi1−/− mice, providing evidence of the influence of Mxi1 on pathways related to IGFBP-3. In addition, Mxi1 inactivation induced cell proliferation *in vivo* and *in vitro*, and regions of proliferation defects, such as cysts, poorly expressed IGFBP-3 in Mxi1−/− mice.

The present study is novel in that it represents the first approach to explain the proliferation mechanism associated with Mxi1. The correlation of Mxi1 and cell proliferation in cancer has been abundantly proven in many studies. However, the regulatory mechanism underlying this correlation has remained elusive. Knowledge of the mechanism is vital if efficacious cancer therapies targeting Mxi1 are to be developed. The present findings are important for this goal.

In summary, the inactivation of Mxi1 suppresses the level of IGFBP-3 and promotes cell proliferation. These mechanisms could be a therapeutic target for cancer caused by Mxi1.

Acknowledgments

This work was supported by National Research Foundation Grant (NRF-2008-314-C00287 and 2010-0029606).

References

[1] K.H. Yoo, Y.N. Kim, M.J. Lee, J.K. Seong, J.H. Park, Identification of apolipoprotein A1 reduction in the polycystic kidney by proteomics analysis of the Mxi1-deficient mouse, Proteomics 9 (2009) 3824–3832.
[2] C.C. Tsao, B.T. Teh, E. Jonasch, N. Shreiber-Agus, E. Efstathiou, A. Hoang, B. Czerniak, C. Logothetis, P.G. Corn, Inhibition of Mxi1 suppresses HIF-2alpha-dependent renal cancer tumorigenesis, Cancer Biol. Ther. 7 (2008) 1619–1627.
[3] N. Schreiber-Agus, Y. Meng, T. Hoang, H. Hou Jr., K. Chen, R. Greenberg, C. Cordon-Cardo, H.W. Lee, R.A. DePinho, Role of Mxi1 in ageing organ systems and the regulation of normal and neoplastic growth, Nature 393 (1998) 483–487.
[4] K. Izumi, D. Kurosaka, T. Iwata, Y. Oguchi, Y. Tanaka, Y. Mashima, K. Tsubota, Involvement of insulin-like growth factor-I and insulin-like growth factor binding protein-3 in corneal fibroblasts during corneal wound healing, Invest. Ophthalmol. Vis. Sci. 47 (2006) 591–598.
[5] M.K. O'Han, R.C. Baxter, L.J. Schedlich, Effects of endogenous insulin-like growth factor binding protein-3 on cell cycle regulation in breast cancer cells, Growth Factors 27 (2009) 394–408.
[6] E. Muhlbradt, E. Asatiani, E. Ortner, A. Wang, E.P. Gelmann, NKX3.1 activates expression of insulin-like growth factor binding protein-3 to mediate insulin-like growth factor-I signaling and cell proliferation, Cancer Res. 69 (2009) 2615–2622.
[7] H.S. Kim, W.J. Lee, S.W. Lee, H.W. Chae, D.H. Kim, Y. Oh, Insulin-like growth factor binding protein-3 induces G1 cell cycle arrest with inhibition of cyclin-

dependent kinase 2 and 4 in MCF-7 human breast cancer cells, Horm. Metab. Res. 42 (2010) 165–172.

[8] K.H. Yoo, Y.H. Sung, M.H. Yang, J.O. Jeon, Y.J. Yook, Y.M. Woo, H.W. Lee, J.H. Park, Inactivation of Mxi1 induces Il-8 secretion activation in polycystic kidney, Biochem. Biophys. Res. Commun. 356 (2007) 85–90.

[9] P.J. Hurlin, J. Huang, The MAX-interacting transcription factor network, Semin. Cancer Biol. 16 (2006) 265–274.

[10] Q.L. Cui, W.H. Zheng, R. Quirion, G. Almazan, Inhibition of Src-like kinases reveals Akt-dependent and -independent pathways in insulin-like growth factor I-mediated oligodendrocyte progenitor survival, J. Biol. Chem. 280 (2005) 8918–8928.

[11] N. Alami, V. Page, Q. Yu, L. Jerome, J. Paterson, L. Shiry, B. Leyland-Jones, Recombinant human insulin-like growth factor-binding protein 3 inhibits tumor growth and targets the Akt pathway in lung and colon cancer models, Growth Horm. IGF Res. 18 (2008) 487–496.

[12] M.L. Neuhouser, J. Schenk, Y.J. Song, C.M. Tangen, P.J. Goodman, M. Pollak, D.F. Penson, I.M. Thompson, A.R. Kristal, Insulin-like growth factor-I, insulin-like growth factor binding protein-3 and risk of benign prostate hyperplasia in the prostate cancer prevention trial, Prostate 68 (2008) 1477–1486.